SCIENCE CHINA
Life Sciences

•RESEARCH PAPER•

https://doi.org/10.1007/s11427-020-1900-7

Abnormal meiosis in fertile and sterile triploid cyprinid fish

Chun Zhang[1†], Qi Li[1†], La Zhu[1], Wangchao He[1], Conghui Yang[1], Hui Zhang[1], Yu Sun[1], Luojing Zhou[1], Yuandong Sun[2], Shurun Zhu[1], Chang Wu[1], Min Tao[1], Yi Zhou[1], Rurong Zhao[1], Chenchen Tang[1] & Shaojun Liu[1*]

[1]*State Key Laboratory of Developmental Biology of Freshwater Fish, College of Life Sciences, Hunan Normal University, Changsha 410081, China;*
[2]*School of Life Sciences, Hunan University of Science and Technology, Xiangtan 411201, China*

Received January 10, 2021; accepted March 9, 2021; published online April 21, 2021

Meiosis is the key process for producing mature gametes. A natural fertile triploid *Carassius auratus* population (3nDTCC) and an artificially derived sterile triploid crucian carp (3nCC) have been previously observed, providing suitable model organisms for investigating meiosis characteristics in triploid fish. In the present study, the microstructures and ultrastructures of spermatogenesis were studied in these fishes. TdT-mediated dUTP nick end labeling detection was performed to investigate the apoptosis of spermatocytes. Fluorescence *in situ* hybridization was employed to trace chromatin pairing. In addition, the mRNA expressions of cell cycle-related genes (i.e., cell division control 2 and cell cycle protein B) were determined by quantitative real-time polymerase chain reaction to illustrate the molecular mechanism of abnormal meiosis in the 3nCC. The results showed that the 3nCC undergoes an irregular prophase I, with the chromosomes distributed in a unipolar radial manner and exhibiting partial pairing, hindered metaphase I, and degenerated cells in the subsequent stages. Meanwhile, the 3nDTCC presented a relatively regular meiotic prophase I with complete conjugate chromosome pairs and chromosomes distributed along the karyotheca, which were presented as a ring structure by slicing. Only the spreads with 130–150 irregular chromosomes can be easily detected in the 3nDTCC, suggesting that it may undergo an abnormal metaphase I. This study provides new insights into the meiosis of fertile and sterile triploid cyprinid fish.

triploid, meiotic configuration, partial pairing, telomere, degenerated cells

Citation: Zhang, C., Li, Q., Zhu, L., He, W., Yang, C., Zhang, H., Sun, Y., Zhou, L., Sun, Y., Zhu, S., et al. (2021). Abnormal meiosis in fertile and sterile triploid cyprinid fish. Sci China Life Sci 64, https://doi.org/10.1007/s11427-020-1900-7

INTRODUCTION

The meiosis of triploid fish with three sets of chromosomes is directly related to the individuals' fertility. In general, triploid individuals are sterile because the three sets of chromosomes cannot be divided evenly during meiosis (Benfey, 1999; Zhang et al., 2005), whereas several triploid fish in natural water systems, such as *Carassius gibelio* (Gui and Zhou, 2010; Zhu et al., 2006) and *Carassius auratus* L. (Xiao et al., 2011; Qin et al., 2016), are fertile, which indicates successful meiosis.

The research on gonad development in triploids is generally focused on microstructural observations of gametogenesis in different stages. However, the relationship between the meiotic configurations of chromosomes and gametogenesis in triploid fish has not been well defined. Early research involving the application of the surface-spreading technique to certain artificial triploid crucian carps revealed an abnormal meiosis; in this case, the pachytene chromosomes were mainly composed of bivalents and unsynapsed univalents (Gui et al., 1995; Zhang et al., 2005).

†Contributed equally to this work
*Corresponding author (email: lsj@hunnu.edu.cn)

The triploid loach produces aneuploid gametes that cannot produce surviving progenies upon crossing (Li et al., 2016). The spermatogenic cells of triploid male *Oncorhynchus mykiss* can complete meiosis but are stagnate in the spermatid stage because nonhomologous chromosomes form irregular synapses, and most of the sperm produced are aneuploid; meanwhile, a small number of spermatogenic cells can develop into normal spermatozoa (Han et al., 2010). Germ cell division is usually unimpeded in natural triploid populations. The triploid crucian carp (*C. gibelio* Bloch) can produce normal mature spermatozoa after meiosis. Their spermatogenesis and the biological activity of spermatozoa are identical to those of diploids (Zhu et al., 2018; Fan et al., 2008). The complete normal meiosis in polyploid *C. gibelio* has also been confirmed by spindle colocalization in mature oocytes and fertilized eggs (Zhang et al., 2015b).

Distant hybridization and subsequent selective breeding lead to an allotetraploid (4*n*=200, abbreviated as 4nAT) population that originated from the red crucian carp (*C. auratus* red var.; RCC)×common carp (*Cyprinus carpio* L.). The artificially derived triploid crucian carp (3nCC) was then obtained by interploidy hybridization between the 4nAT (male) and improved diploid RCC (female) (Liu et al., 2001; Liu, 2010). The 3nCC fish are sterile given that the testes of males do not produce normal sperm. Instead, their germ cells develop into round spermatids and subsequently degenerate (Liu et al., 2000). The transcriptome analysis of the testis has also shown that the apoptotic pathway plays a central role in the sterility of male triploid fish (Xu et al., 2015). A natural triploid crucian carp (*C. auratus* L.; 3nDTCC) in the Dongting water system in China was previously reported by our group. The male and female 3nDTCC are similarly fertile and produce bisexual triploid offspring when mating with each other (Xiao et al., 2011). The sterile triploid 3nCC and fertile triploid 3nDTCC provide excellent resources for the analysis of the meiotic configuration of triploid fish.

In the present study, we examined the meiotic configuration of male 3nDTCC and 3nCC by observation of their microstructure and ultrastructure, validation by quantitative real-time polymerase chain reaction (qPCR), and analysis of fluorescence *in situ* hybridization (FISH). Furthermore, to analyze the fertility of the triploids, we detected the DNA contents of the 3nDTCC sperm and performed TdT-mediated dUTP nick end labeling (TUNEL) on the male triploid tissue. The results of this study can elucidate the different meiotic configurations of fertile naturally occured triploids and sterile artificially derived triploids and provide new insights into why specific triploid fish are fertile, and others are not.

RESULTS

Seasonal characteristics of all samples

Five individuals from 3nDTCC and 3nCC were sampled at 6–7, 8–10, 11–12, and 13–18 months. The number of spermatocyte chromosome spreads in the air-dried slides differed depending on the age (Table 1). A high incidence of meiotic spreads generally occurred in the 3nDTCC samples aged 11–12 months and in the 3nCC samples aged >6 months. The cells of 3nDTCC and 3nCC aged 12 months were selected to compare these division characteristics via cytological, ultrastructural, and spermatocyte chromosome spread observation. The 3nDTCC cells at 12 months were used to detect the DNA content of sperm.

3nDTCC males are fertile, whereas 3nCC males are sterile

Microscopic detection revealed that the 3nDTCC males can produce white semen with good sperm motility during the breeding season. By contrast, the 3nCC males cannot produce mature spermatozoon throughout their lifetime. Significant differences in the cell morphology and cell composition of 3nDTCC and 3nCC were found during spermatogenesis. The quantitative morphometric analysis of testis tissue components revealed differences post-spermatogenesis. Spermatids and spermatozoa were visible in the 3nDTCC but completely absent in the 3nCC. Several degenerated spermatocytes were found in the 3nDTCC, whereas 3nCC showed a strong accumulation of degenerated spermatocytes (Figure 1A–D). The characteristics of meiotic division differed between 3nDTCC and 3nCC. Table S1 in Supporting Information shows the detailed and annotated information of Figure 1C.

Table 1 Introduction of sample characteristics

Samples	Weight (g)	Semen produced or not	The incidence of chromosome spreads of spermatocytes in air-drying slides
3nDTCC at 6–7 months	30±5	No	few
3nDTCC at 8–10 months	60±5	yes	few
3nDTCC at 11–12 months	120±5	yes	rich
3nDTCC at 13–18 months	150±5	yes	few
3nCC at 6–7 months	50±5	No	rich
3nCC at 8–12 months	350±10	No	rich

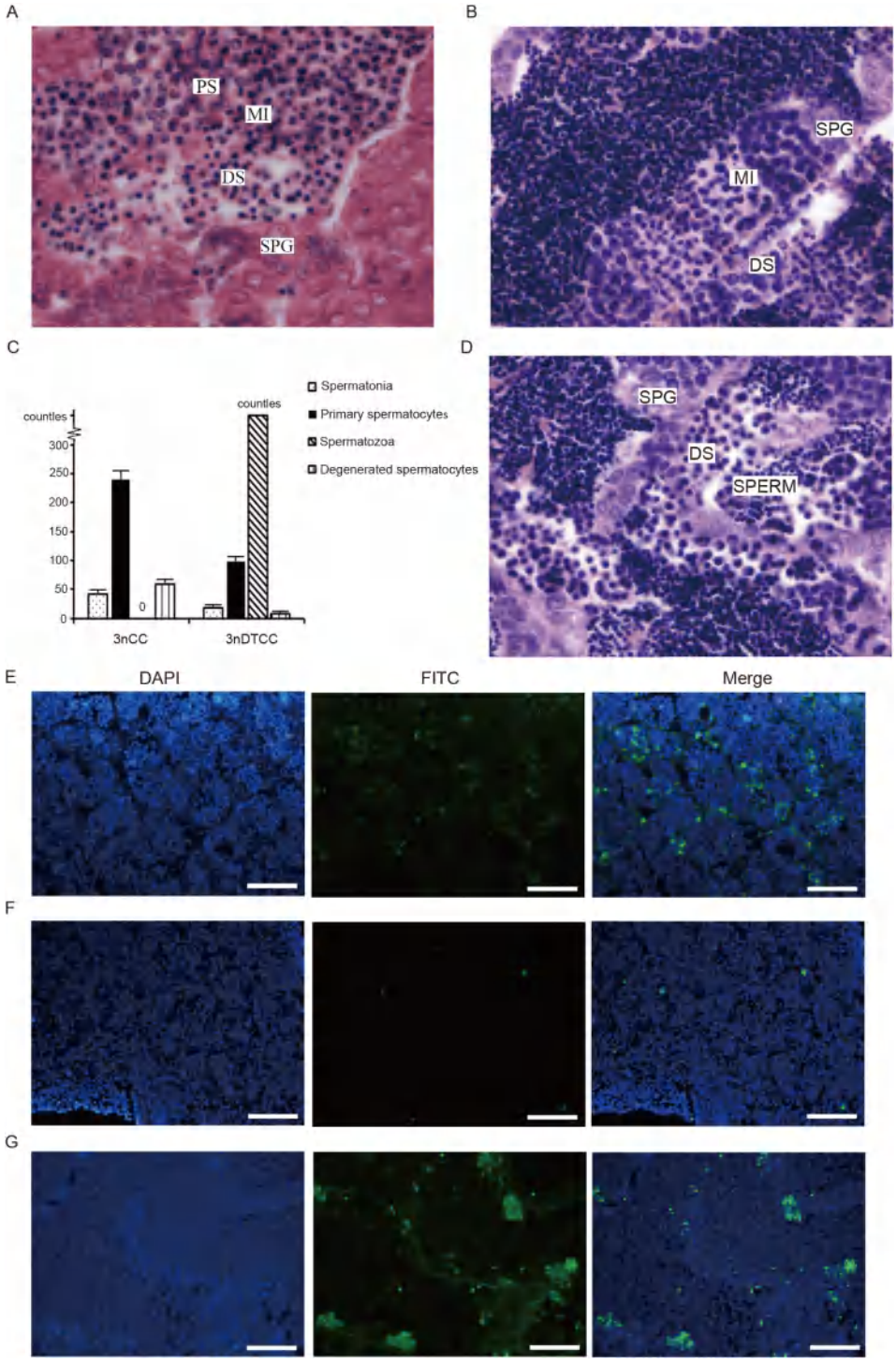

Figure 1 Testis histology and TUNEL staining of 3nCC and 3nDTCC. A, B and D, Cell morphology and cell composition of seminiferous tubules in (A) 3nCC and (B and D) 3nDTCC. SPG: Spermatogonia, PS: primary spermatocytes, MI: meiosis I; DS: degenerated spermatocytes. C, Morphometric analysis of testis sections. 3nCC showed high incidences of spermatogonia, primary spermatocytes, and degenerated spermatocytes but not spermatozoa (sperm), whereas 3nDTCC showed high incidences of spermatozoa and spermatocytes with several spermatogonia and apoptotic cells. TUNEL staining of (E) 3nCC and (F and G) 3nDTCC. E, High incidence of degenerated spermatocytes in 3nCC. F, 3nDTCC testes showed extremely low levels of apoptosis. G, Several individuals in 3nDTCC revealed high levels of apoptosis. Bar=30 μm.

The degenerated spermatocytes showed highly condensed nuclei and were presumed to be undergoing apoptosis. The high incidence of degenerated spermatocytes in the 3nCC was confirmed by TUNEL staining (Figure 1E). Although the cells from the 3nDTCC testes showed extremely low levels of apoptosis (Figure 1F), several individuals exhibited high levels of apoptosis (Figure 1G).

Meiotic I division in 3nDTCC and 3nCC

Morphological changes in the nuclear division during the different substages of meiosis I were observed in the primary spermatocytes of 3nDTCC and 3nCC by histological sections. In the meiotic prophase I of the 3nCC, the chromosomes of primary spermatocytes were distributed in a unipolar radial manner and showed in the cross-section view with a pyknotic pattern in an irregular semicircle along the karyotheca. In metaphase I, regular spindles and dark equatorial-plate chromosomes were observed. The metaphase chromosomes cannot be separated on the poles, resulting in condensed and degenerated spermatocyte nuclei (Figure 2A, C, E, G, and I). By comparison, during meiotic prophase I of the 3nDTCC, the chromosomes of the primary spermatocytes were concentrated along the karyotheca and presented as a regular ring in the cross-section view. In metaphase I, the equatorial-plate chromosomes were observed in the primary spermatocytes. Finally, in anaphase I, the chromosomes were pulled by spindles and split between the two poles (Figure 2B, D, F, H, and J).

Ultrastructures of testes from 3nDTCC and 3nCC

Electron microscopy of the testes showed that the meiotic characteristics of 3nCC and 3nDTCC germ cells evidently differed from those of zygotene-stage cells. Fine fibroid chromosome structures were observed in the nuclei of zygotene-stage spermatocytes in the 3nCC. Telomeres with specific movement routines were attached to the nuclear membrane, and either double-linear or single-linear chromosomes can be found. The double-linear chromosomes may indicate the synapsis and pairing of chromosomes, whereas the single-linear chromosomes may indicate unpaired chromosomes (Figure 3A and C). By comparison, all the fine fibroid chromosomal structures in the nuclei of zygotene-stage spermatocytes of the 3nDTCC were paired in a double-linear manner (Figure 3B and D). During metaphase I and anaphase I of the 3nCC, most chromosomes were blocked at the equatorial plate, and several chromosomes were pulled to the poles by spindles (Figure 3E). By comparison, during meiotic metaphase I of the 3nDTCC, the homologous chromosomes were concentrated on the equatorial plate (Figure 3F), and the ultrastructures of the 3nDTCC meiotic cells in anaphase I was not observed temporarily. The spermatocyte nucleus of the 3nCC was blocked in metaphase I, and the nuclear material gradually condensed to form a solid spermatocyte nucleus, whose diameter was significantly larger than the head of mature sperm (Figure 3G and I). The 3nDTCC can successfully proceed through meiosis and produce sperm cells. The nuclear materials of the 3nDTCC were either marginalized and agglutinated under the nuclear membrane to form loops (red arrow) or gradually condensed into clumps (blue arrow) (Figure 3H) and then continued to form mature sperm surrounded by flagellar structures (Figure 3J).

Chromosome spread during meiosis I in 3nCC and 3nDTCC

Meiosis progression significantly differed between 3nCC and 3nDTCC. During the early stages of meiosis in the 3nCC, half of the chromosomes in zygotene-stage cells were thick, but others were thin (Figure 4A). When the cells entered the metaphase of meiosis I, 50 pairing bivalents and 50 unsynapsed univalents were observed. Here, several pairing bivalents presented specific characteristics, suggesting two telomere connection loci, such as a ring, whereas others presented one telomere connection locus (Figure 4B). In the 3nDTCC, the chromosomes in zygotene-stage cells showed a uniform thickness (Figure 4C). When the cells entered the metaphase of meiosis I, no classical bivalent chromosomes were observed. Only the spreads with 130–150 irregular chromosomes were easily detected; this finding contradicts the previous observations on conventional bivalents in common diploid fish (Figure 4D). Table 2 shows the distribution of bivalents or chromosome numbers during meiosis I of all the samples.

The RCC is an allotetraploid fish containing two subgenomes (AABB) (Chen et al., 2019; Chen et al., 2020; Luo et al., 2020). The subgenomes of this fish were previously detected by 5S rDNA FISH, and two strong signals of the 5S rDNA probes were located in the first submetacentric chromosome pair of the RCC. Several weak signals located in other chromosomes were also noted. By comparison, the common carp showed no such major signals (Zhang et al., 2015a; Ye et al., 2017). Three strong signals, indicating three sets of genomes, and three weak signals of 5S rDNA have been observed in the 3nDTCC (Qin et al., 2016). Given the lack of distinct rules on the number of weak signals in the current research, we focused on the strong signals of the 5S rDNA to infer the chromosome composition of the RCC in this paper. The 263 bp centromere probes were localized to all 100 chromosomes in the RCC but to none of those in common carp (Qin et al., 2014). These probes were used to detect the chromosomal pairing characteristics of 3nCC and 3nDTCC in the present study.

The 5S rDNA localization in chromosome spreads in metaphase I of the 3nCC showed two strong signals in a pair of chromosomes and several weak signals in other chromosomes. These chromosomes were considered bivalents originating from two sets of RCC genome pairings (Figure 4E, yellow box). The localization of the 263 bp centromere probe in the chromosome spreads in metaphase I of the 3nCC indicated 80–100 centromere loci, in which several signals were paired, and the other signals were not (Figure 4F). The

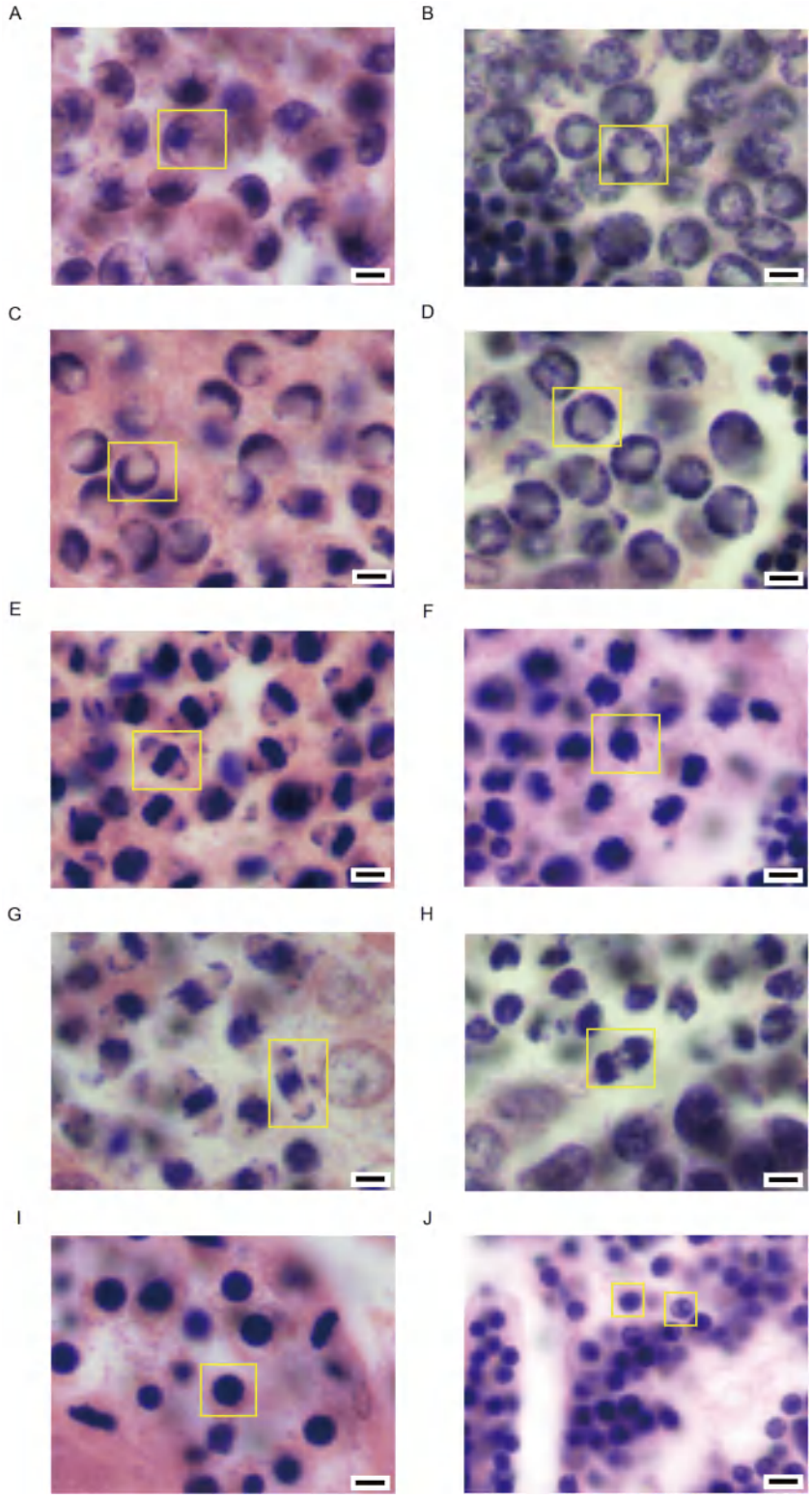

Figure 2 Detection of morphological changes during meiotic division at different substages of meiosis I-stage spermatocytes in 3nDTCC and 3nCC by histological examination. A–D, In prophase I, the chromosomes were distributed (A) in a unipolar radial manner in the 3nCC but (B) formed a ring along the karyotheca in 3nDTCC. Thereafter, the chromosomes (C) showed pyknosis in an irregular semicircle along the karyotheca in the 3nCC but (D) condensed into regular rings in the 3nDTCC. E, In metaphase I, regular spindles and dark equatorial-plate chromosomes were observed in the 3nCC. F, Equatorial-plate chromosomes were observed in the 3nDTCC primary spermatocytes. G and I, The metaphase chromosomes of the 3nCC (G) cannot be separated between the poles; they (I) condensed and degenerated to form a dense spermatocyte nucleus, which had a significantly larger diameter than the sperm head. H, Chromosomes of the 3nDTCC were separated on the poles under spindle traction and (J) further developed into mature sperm. The mature sperm of 3nDTCC is shown in the left frame, and a spermatid in the process of maturation is shown in the right frame. Bar=4 μm.

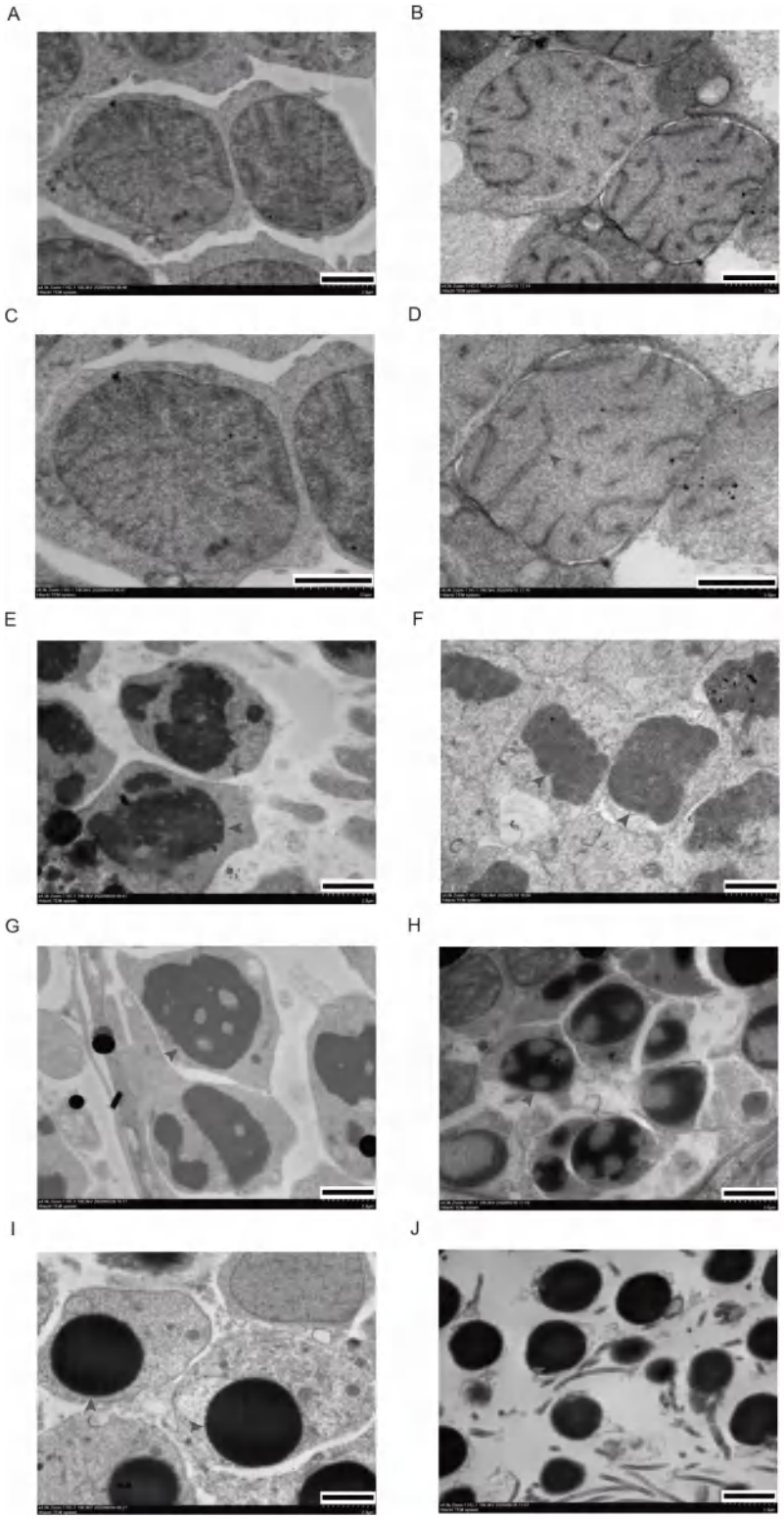

Figure 3 The ultrastructures of testes from 3nDTCC and 3nCC. A and B, Zygotene-stage cells of (A) 3nCC and (B) 3nDTCC. C, The red arrow shows the unpaired chromosome of the 3nCC, and the blue arrow shows the synapsis and pairing chromosome of the 3nCC. D, The blue arrow shows the synapsis and pairing chromosome of the 3nDTCC. E, During metaphase I and anaphase I of the 3nCC, most chromosomes were blocked at the equatorial plate, and several chromosomes were pulled to the poles by the spindles. F, During metaphase I of the 3nDTCC, the homologous chromosomes were focused on the equatorial plate. G, The spermatocyte nucleus of the 3nCC was condensed. H, The spermatocyte nuclear chromosomes of the 3nDTCC were either marginalized and agglutinated under the nuclear membrane to form loops (red arrow) or gradually condensed into clumps (blue arrow). I, The spermatocyte nucleus of the 3nCC was completely condensed and formed a solid spermatocyte nucleus with a diameter significantly larger than that of the head of mature sperm. J, The spermatozoa of 3nDTCC were formed, and flagellar structures were observed. Bar=2 μm.

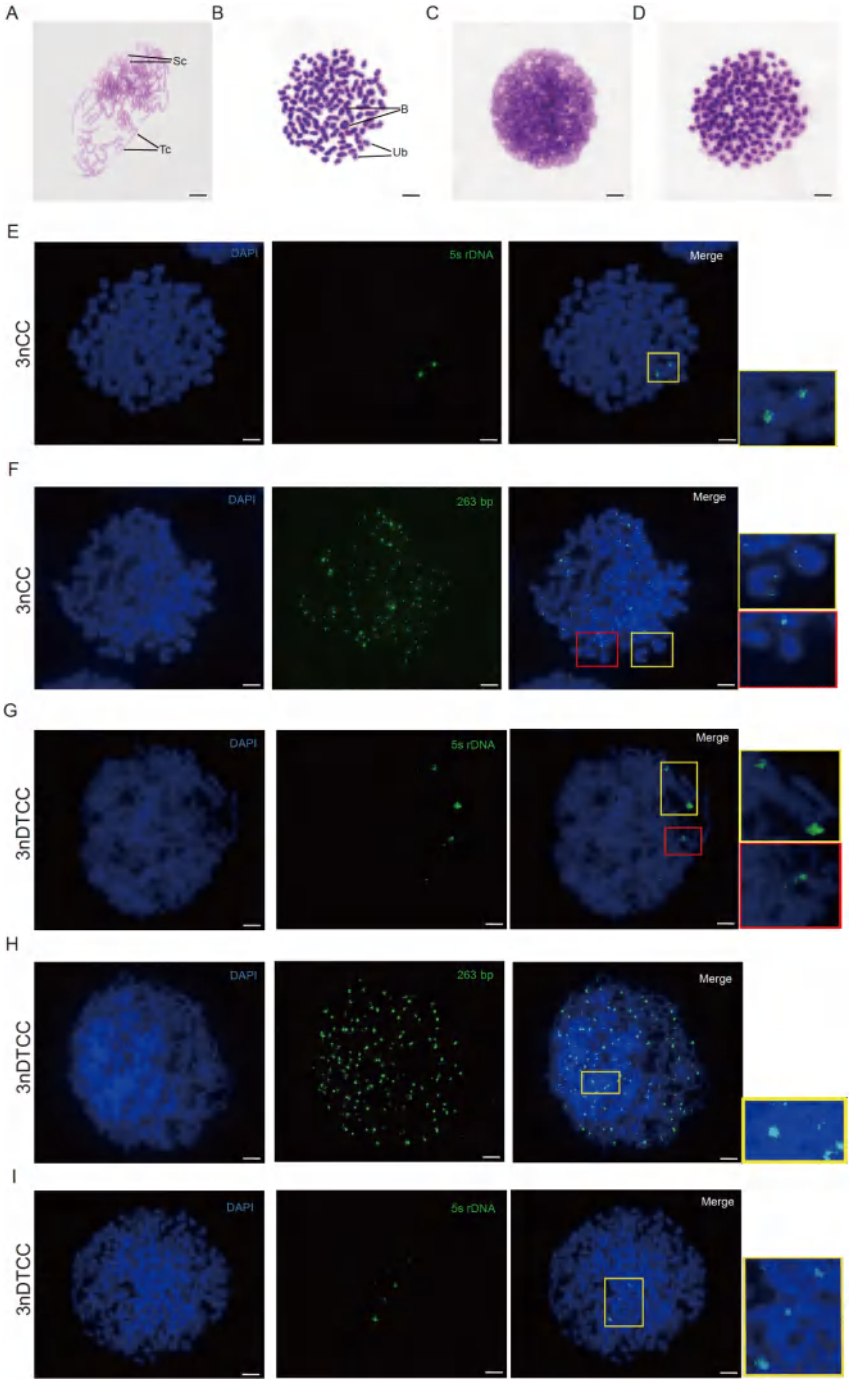

Figure 4 Meiosis chromosome spreads and FISH of 3nCC and 3nDTCC. A, Chromosome spread of zygotene-stage cells in the 3nCC. Sc: slim chromosome; Tc: thick chromosome. B, Chromosome spread of metaphase I-stage cells in the 3nCC. B: bivalent. Ub: univalent. C, Chromosome spread of zygotene-stage cells in the 3nDTCC. D, Chromosome spread of meiosis I-stage cells in the 3nDTCC. E, 5S rDNA localization in metaphase I-stage cells of the 3nCC. The box indicates two signals located on a pairing bivalent. F, The 263 bp centromere repeat sequence localization in metaphase I-stage cells of the 3nCC. The yellow box indicates pairing signals. G, 5S rDNA localization in the zygotene-stage cells of the 3nDTCC. The yellow box shows two paired signals (i.e., a pair of homologous chromosomes joined with a telomere connection locus), and the red box shows a single visible signal. H, The 263 bp centromere repeat sequence localization in the zygotene-stage cells of the 3nDTCC. The chromosome signals were not counted and presumed to occur in pairs. The yellow box indicates the pairing of strong signals, such as overlapping double signals, and several weak signals. I, 5S rDNA localization in chromosome spreads with 130–150 irregular chromosomes of the 3nDTCC showing three strong signals. Bar=3 μm.

5S rDNA localization in chromosome spreads during the meiosis of 3nDTCC was observed in cells at the zygotene stage and showed one pair of strong signals (yellow box, a pair of homologous chromosomes with two signals joined with one telomere connection locus) and a single strong signal (red box) in all the detected spreads (Figure 4G). The results may indicate the pairing of the three sets of crucian carp chromosomes. Here, paired strong signals imply pairing

Table 2 Distribution of bivalents or chromosome numbers during meiosis I in 3nCC and 3nDTCC

Fish type	Sample number	Spread number	Bivalent or chromosome number				
			50II+50I	other	135–149	150	151–160
3nCC	3	60	48	12			
3nDTCC	3	70		10	5	39	16

between two homologous chromosomes, and a single strong signal means the pairing between two nonhomologous chromosomes. Furthermore, the localization of the 263 bp centromere repeat sequence in the zygotene-stage cells of 3nDTCC showed that chromosome signals were not counted and presumed to occur in pairs. Several strong signals, such as overlapping double signals, and several weak signals were also notably paired (Figure 4H). The 5S rDNA localization in spreads with 130–150 irregular chromosomes of the 3nDTCC showed three strong signals (Figure 4I). Table 3 shows the FISH data.

DNA content of sperm in 3nDTCC

Between the two studied fish, only the 3nDTCC can produce semen. Thus, the DNA content of semen collected from 10 3nDTCC males was detected by flow cytometry. The blood cells of the 3nDTCC were used as controls. The results showed that all samples produced a major peak at approximately 3C DNA content, which means that the peak represented 1.5*n* sperm (Figure 5A and B).

qPCR validation

The *cdc2* can combine with *cyclinB* to form the maturation promoting factor (MPF) and then initiate G2→M phase transition. The expression levels of *cdc2* and *cyclinB* can well explain the cell cycle state of the 3nCC germ cells. qPCR showed that the expression levels of these genes were higher in the 3nCC than in the 3nDTCC (Figure 6) because the 3nCC germ cells were inhibited in metaphase I, which led to the spermatocyte accumulation in this phase. The relevant genes maintaining the metaphase stage presented high mRNA expression levels. By contrast, the 3nDTCC germ cells were not hindered during meiosis and easily crossed the metaphase stage with minimal aid from MPF. These results indicate that the spermatocytes of 3nCC are inhibited in metaphase I at the molecular level.

DISCUSSION

Several methods, including natural spontaneous occurrence and artificial induction, are used to produce triploid fish. In the natural triploid fish group, the chromosomes in germ cells of several species show incomplete pairing, with numerous univalents observed during the pachytene stage. The triploid *Trichomycterus davisi* can produce fertile sperm (Borin et al., 2002). Another natural triploid fish, *C. gibelio,* can produce normal mature 1.5*n* spermatozoa after normal meiosis, although no specific details about its meiosis configuration are available (Fan et al., 2008). Different methods have been developed to induce artificial triploid fish cases. Various artificial triploid cases were induced by inhibiting the release of secondary polar bodies immediately after fertilization. The artificially induced triploid loach (*Misgurnus anguillicaudatus*) generates an unusual 1.5*n* aneuploid spermatozoa; in this way, in these spermatozoa, approximately 25 bivalents and 25 univalents (abbreviated 25IIs and 25Is, respectively) in the cells at the pachytene stage can be observed (Zhang and Arai, 1999). The artificially induced triploid rainbow trout (*O. mykiss*) generates 1*n*, 1.5*n*, 2*n*, and other aneuploid spermatozoa; here, the vast majority of spermatogenic cells are in diapause at the spermatid stage, the nonhomologous chromosome in spermatocytes undergoes irregular synapses, and a small number of spermatogenic cells develop into normal spermatozoa (Han et al., 2010). Another artificially induced triploid fish case presents as a hybrid, including an autotriploid hybrid between an autotetraploid and diploid, and an allotriploid hybrid between a tetraploid and diploid. The meiotic cells of the autotriploid hybrid of *M. anguillicaudatus* frequently exhibit 25IIs and 25Is and produce 1.5*n* and other aneuploid spermatozoa, which can be predicted to result from the equal segregation of 25IIs and random segregation of 25Is (Li et al., 2016). An allotriploid crucian carp fish has been produced by crossing male allotetraploids originating from the RCC (*C. auratus* red var.)×common carp (*C. carpio* L.) with a female Japanese crucian carp. Here, 50IIs and 50Is were observed at the pachytene-stage cells, and no mature spermatozoa were noted (Zhang et al., 2005).

In this paper, the evidence of an abnormal meiotic configuration in the artificial 3nCC, which is sterile, was found. As shown in Figures 3 and 4, the 3nCC produced by artificial hybridization cannot normally complete meiosis and form mature sperm, with abnormal division characteristics being observed in prophase I. The chromosomes of zygotene-stage cells in the 3nCC were condensed to one pole along the nuclear membrane; here, some chromosomes were attached to the nuclear membrane with the chromosomal telomeres and some chromosomes lost attaching. Half of the chromosomes were thick, whereas the others were thin. Then, the

Table 3 Examination of localization signals by FISH in the meiotic chromosome spreads of 3nCC and 3nDTCC

Probe type	Fish type	Sample number	Spread number	Bivalent or chromosome number	Number of loci	Note
5S rDNA probe	3nCC	5	100	50II+50I	2	Two signals located in a pair of chromosomes
	3nDTCC	5	100	130–150	3	Two signals located in a pair of chromosomes, and 1 signal located in the other pair of chromosomes
				130–150	3	Three strong signals distributed separately
263 bp centromere probe	3nCC	5	100	50II+50I	80–100	Some pairing signals
	3nDTCC	5	100	130–150	>100	The signals presumed to come in pairs

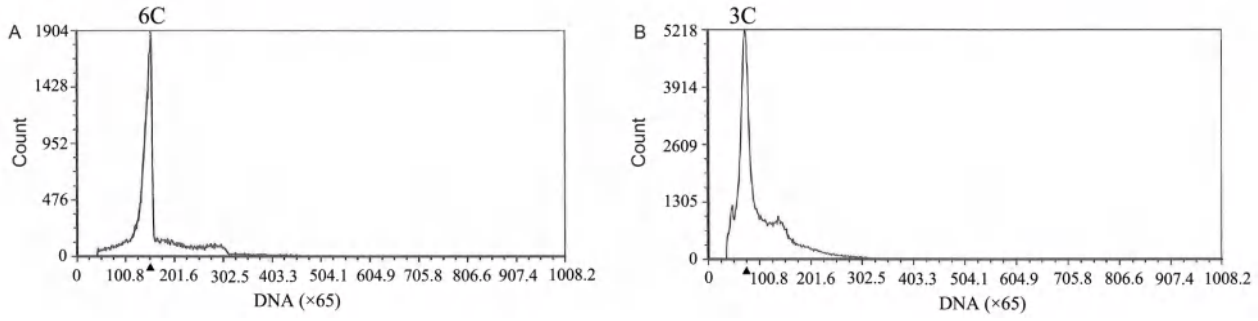

Figure 5 Flow cytometry histograms of semen cells obtained from the 3nDTCC. The blood cells of the 3nDTCC were detected as the control. A, Blood cells of the 3nDTCC-1 (DNA content, 6C). B, Semen cells of the 3nDTCC-1 (DNA content, 3C).

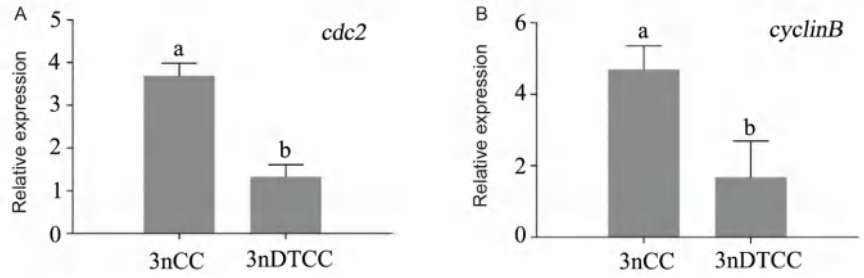

Figure 6 Real-time PCR analysis of *cdc2* and *cyclinB* in 3nCC and 3nDTCC. A, *cdc2*, cell division control 2. B, *cyclinB*, cell cycle protein B. The different lowercase letters in each panel indicate significant differences at $P<0.05$ (mean±standard deviation of relative expression; $n=9$ for each group).

chromosomes of metaphase I-stage cells in the 3nCC presented bivalents and univalents. The FISH of 5S rDNA and 263 bp centromere repeat sequences demonstrated the partial pairing of chromosomes in metaphase I, which can lead to the abnormal separation and inhibition of homologous chromosomes in this phase. The strongest evidence of abnormal meiosis of the 3nCC was obtained through slice observation: chromosomes on the equatorial plate cannot be separated on the poles in metaphase I, resulting in the high expressions of *cdc2* and *cyclinB*. Thereafter, spermatocyte apoptosis, pyknosis, and degeneration occurred. The above findings imply that spermatocytes in the 3nCC are easily inhibited in metaphase I. Thus, secondary spermatocytes, spermatids, or sperm cannot be easily generated.

Similar to previous studies on diploid fish, the naturally triploid 3nDTCC can produce primary spermatocytes, secondary spermatocytes, spermatids, and sperm. In prophase I-stage spermatocytes of the 3nDTCC, early chromosomes are normally distributed along the nuclear membrane, and the chromosomal telomeres remain in contact with the nuclear membrane. In addition, given the chromosomes of zygotene-stage cells in 3nDTCC pair between two homologous chromosomes or two nonhomologous chromosomes (Figure 4G and H), we can preliminarily conclude that synapsis occurs between two chromosomes and not among three chromosomes. Furthermore, the DNA content detection in the 3nDTCC sperm showed the reduced production of 1.5*n* sperm, which further verified the same point.

According to the above results, the 3nCC may be assumed incapable of undergoing normal chromosome pairing because of the composition of its three sets of allochromosomes, which can initially influence the movement routines

of telomeres or their attachment to the nuclear envelope. Thus, an irregular prophase I process occurred in the 3nCC, with chromosomes being distributed in a unipolar radial manner (Figure 2A and C) and exhibiting partial pairing, which led to the inhibition of primary spermatocytes during the metaphase of meiosis I and their eventual degeneration. By contrast, the 3nDTCC can perform normal homologous chromosome pairing due to the origin of autopolyploids (Qin et al., 2016). The chromosomal telomeres of the 3nDTCC possess normal movement routines and maintain attachment to the nuclear envelopes; this process ensures that the 3nDTCC undergoes normal chromosomal synapsis, and that the chromosomes distribute along the nuclear envelope, forming a ring shape in the cross-section view in early prophase I (Figure 2B and D). Chromosomal telomeres attaching to the nuclear envelope provide an ordered orbit for the chromosome synapses. These findings provide a new perspective for the analysis of the mechanism of triploid sterility and require further study.

Only spreads with 130–150 irregular chromosomes were easily observed, which contradicts the previous findings on bivalent elements in common diploid fish. We speculate that capturing chromosomal spreads at the stages of diplotene, diakinesis, and paired metaphase I is difficult, and that these spreads may originate from anaphase I-stage spermatocytes, the chromosome spread of which showed three strong signals in the 5S rDNA FISH. The reasons for the difficulty in capturing these stages in the 3nDTCC require further study. We speculate that the meiosis of homologous triploid pairs may not require normal cross-termination, which can lead to an extremely short or absence of cross-termination during diplotene or diakinesis. Borin LA also suggested the absence of synapsis in triploid *T. davisi* (Borin et al., 2002).

The 3nDTCC is generally propagated by gynogenesis. The sperms of the 3nDTCC mostly activate triploid ova and do not participate in the genetic makeup of offspring (Li et al., 2014; Zhu et al., 2018; Li and Gui, 2018); thus, the requirements for the ploidy integrity of sperm are not as high as those for syngamy diploids. Thus, a precise conventional meiosis mechanism may not be required to ensure the genetic material integrity of sperms. Therefore, the unique meiosis of the male 3nDTCC may be related to the adaptive evolution of gynogenetic fish, which is worthy of further investigation.

MATERIALS AND METHODS

Experimental fish

Male triploid 3nDTCC and 3nCC aged 6–7 and 10–11 months, respectively, were collected from the State Key Laboratory of Developmental Biology of Freshwater Fish, Hunan Normal University. Animal experimenters were certified under a professional training course for laboratory animal practitioners held by the Institute of Experimental Animals, Hunan Province, China. All of the fish were euthanized using 2-phenoxyethanol (Sigma-Aldrich, USA) before being dissected. The fish were treated humanely following the regulations of the Administration of Affairs Concerning Experimental Animals for the Science and Technology Bureau of China. All applicable institutional and national guidelines for the care and use of animals were followed.

Histology

The testes of five randomly selected individuals of the two kinds of triploid fish of different ages were collected and fixed in Bouin's solution for tissue section preparation. The paraffin-embedded sections were cut, stained with hematoxylin and eosin, and observed under a Pixera Pro 600Es microscope (Pixera, USA).

The TUNEL detection was performed on tissues fixed in 4% paraformaldehyde. Then, the tissues were embedded in paraffin and sectioned to a thickness of 5 mm. A commercial *in situ* cell death detection kit (One Step TUNEL Apoptosis Assay Kit, Beyotime, Shanghai, China) was used. The tissue sections were deparaffinized in xylene for 20 min and hydrated through a graded ethanol series. Then, the tissue sections were treated with proteinase K solution for 10 min and incubated in the TUNEL reaction mixture for 1 h at 37°C in a humidified chamber. After TUNEL staining, the sections were counterstained with 4′,6-diamidino-2-phenylindole (DAPI) to label all nuclei. A blue staining indicated the DAPI-stained nuclei, whereas the green staining indicated the TUNEL-positive cells.

Electron microscope analysis of spermatogenesis

Testis tissue samples were collected, fixed in 3% glutaraldehyde solution, washed with phosphate buffer, transferred to an osmic acid solution, dehydrated in a graded acetone series, and embedded in Epon812. Ultrathin sections were cut and stained with uranyl acetate and lead citrate. An HT7800 transmission electron microscope (HITACHI, Japan) was used to observe the ultrastructures of the tissues.

FISH of spermatocyte chromosome spreads

The chromosomal locations of the 5S rDNA of the triploid 3nDTCC and 3nCC were analyzed by FISH. Chromosome preparations were performed by air-drying preparation technology as previously described (Zhang et al., 2015a). Testis tissues were hypotonically collected and fixed, and the spermatocyte cells were spread on clean slides. FISH was performed in accordance with a previously described method

(Zhang et al., 2015a). The FISH probes included a 340 bp 5S rDNA repeat sequence and a 263 bp centromere repeat sequence amplified from the genomic DNA of the RCC and labeled with Dig-11-dUTP using a PCR DIG Probe Synthesis Kit (Roche, Germany). The 340 bp 5S rDNA repeat sequence was amplified by PCR using the following primer pairs: 5′-TATGCCCGATCTCGTCTGATC-3′ and 5′-CAGGTTGGTATGGCCGTAAGC-3′ (sequence number KM359663). The 263 bp centromere repeat sequence was amplified by PCR using the primer pairs: 5′-AAGCTTTTCTCTCTAGTAGAGAAAGC-3′ and 5′-TTGAGCAGATTTGGGCTTGATTTC-3′ (sequence number JQ086761). The slides were viewed under a Leica inverted DMIRE2 microscope image system (Leica, Germany). The images were captured using the CW4000 FISH software (Leica).

Measurement of DNA content

A flow cytometer (Partec GmbH, Germany) was employed to detect the sperm ploidy of the 3nDTCC. Spermatic fluid samples were squeezed out from the mature male 3nDTCC (5–10 μL per fish), and sperm motility was detected under a microscope. The fluid was then treated with DAPI DNA staining solution for 10–15 min and filtered. The DNA content of the red blood cells from the 3nDTCC was used as a control.

qPCR analysis

The cell cycle-related genes (i.e., cell division control 2 (*cdc2*) and cell cycle protein B (*cyclinB*)) involved in testis development were selected for verification and comparison of 3nCC and 3nDTCC using qPCR. The total RNA was extracted from the remaining testicular tissue and reverse transcribed into first-strand cDNA using reverse transcriptase (Invitrogen, USA). Real-time PCR was performed using the Prism 7500 Sequence Detection System (Applied Biosystems, USA) with PowerUp™ SYBR™ Green Master Mix (Applied Biosystems). Real-time qPCR was performed in triplicates.

The reaction mixture (10 μL) consisted of the following components: 2.5 μL cDNA (1:4 dilution), 5 μL PowerUp™ SYBR™ Green Master Mix, 0.5 μL specific forward primers, 0.5 μL reverse primers, and 1.5 μL water. The amplification conditions were 50°C for 5 min and 95°C for 10 min, followed by 40 cycles at 95°C for 15 s and 60°C for 45 s. The average threshold cycle (C_t) was calculated for each sample using the $2^{-\Delta\Delta C_t}$ method and normalized to β-actin. Finally, a melting curve analysis was performed to validate the specific amplification of the expected products.

Compliance and ethics *The author(s) declare that they have no conflict of interest.*

Acknowledgements *This work was supported by the National Natural Science Foundation of China (31873038, 31730098 and U19A2040), the earmarked fund for the China Agriculture Research System (CARS45), Key Research and Development Program of Hunan Province (2017NK1031), and 111 project (D20007).*

References

Borin, L.A., Martins-Santos, I.C., and Oliveira, C. (2002). A natural triploid in *Trichomycterus Davisi* (Siluriformes, Trichomycteridae): mitotic and meiotic characterization by chromosome banding and synaptonemal complex analyses. Genetica 115, 253–258.

Benfey, T.J. (1999). The physiology and behavior of triploid fishes. Rev Fish Sci 7, 39–67.

Chen, Z., Omori, Y., Koren, S., Shirokiya, T., Kuroda, T., Miyamoto, A., Wada, H., Fujiyama, A., Toyoda, A., Zhang, S., et al. (2019). *De novo* assembly of the goldfish (*Carassius auratus*) genome and the evolution of genes after whole-genome duplication. Sci Adv 5, eaav0547.

Chen, D., Zhang, Q., Tang, W., Huang, Z., Wang, G., Wang, Y., Shi, J., Xu, H., Lin, L., Li, Z., et al. (2020). The evolutionary origin and domestication history of goldfish (*Carassius auratus*). Proc Natl Acad Sci USA 117, 29775–29785.

Fan, Z.T., Yang, J., Chen, W.X., and Chen, S.B. (2008). Spermatogenesis in triploid and diploid of crucian carps *Carassius auratus gibelio* (in Chinese). Acta Zool Sin 54, 467–474.

Gui, J.F., Chen, L., Liang, S.C., and Jiang, Y. (1995). Light microscopy of meiosis chromosome pairing in artificial triploid fish with ovarian development retardation (in Chinese). Acta Hydrobiol Sin 19, 223–226.

Gui, J.F., and Zhou, L. (2010). Genetic basis and breeding application of clonal diversity and dual reproduction modes in polyploid *Carassius auratus gibelio*. Sci China Life Sci 53, 409–415.

Han, Y., Liu, M., Zhang, L.L., and Li, H.L. (2010). Research on reproduction and development of triploid male *Oncorhynchus mykiss* (in Chinese). J Northeast Agric Univ 41, 94–99.

Li, X.Y., Zhang, X.J., Li, Z., Hong, W., Liu, W., Zhang, J., and Gui, J.F. (2014). Evolutionary history of two divergent *Dmrt1* genes reveals two rounds of polyploidy origins in gibel carp. Mol Phylogenets Evol 78, 96–104.

Li, X.Y., and Gui, J.F. (2018). Diverse and variable sex determination mechanisms in vertebrates. Sci China Life Sci 61, 1503–1514.

Li, Y.J., Gao, Y.C., Zhou, H., Ma, H.Y., Lin, Z.Q., Ma, T.Y., Sui, Y., and Arai, K. (2016). Aneuploid progenies of triploid hybrids between diploid and tetraploid loach *Misgurnus anguillicaudatus* in China. Genetica 144, 601–609.

Liu, S.J. (2010). Distant hybridization leads to different ploidy fishes. Sci China Life Sci 53, 416–425.

Liu, S.J., Hu, F., and Zhou, G.J. (2000). Observation on the gonad structure of improved triploid crucian carp in reproduction season (in Chinese). Acta Hydrobiol Sin 24, 301–306+405–406.

Liu, S., Liu, Y., Zhou, G., Zhang, X., Luo, C., Feng, H., He, X., Zhu, G., and Yang, H. (2001). The formation of tetraploid stocks of red crucian carp×common carp hybrids as an effect of interspecific hybridization. Aquaculture 192, 171–186.

Luo, J., Chai, J., Wen, Y., Tao, M., Lin, G., Liu, X., Ren, L., Chen, Z., Wu, S., Li, S., et al. (2020). From asymmetrical to balanced genomic diversification during rediploidization: Subgenomic evolution in allotetraploid fish. Sci Adv 6, eaaz7677.

Qin, Q., Wang, Y., Wang, J., Dai, J., Liu, Y., and Liu, S. (2014). Abnormal chromosome behavior during meiosis in the allotetraploid of *Carassius auratus* red var. (♀)×*Megalobrama amblycephala*(♂). BMC Genet 15, 95.

Qin, Q., Wang, J., Hu, M., Huang, S., and Liu, S. (2016). Autotriploid origin of *Carassius auratus* as revealed by chromosomal locus analysis. Sci China Life Sci 59, 622–626.

Xiao, J., Zou, T., Chen, Y., Chen, L., Liu, S., Tao, M., Zhang, C., Zhao, R., Zhou, Y., Long, Y., et al. (2011). Coexistence of diploid, triploid and

tetraploid crucian carp (*Carassius auratus*) in natural waters. BMC Genet 12, 20.
Xu, K., Wen, M., Duan, W., Ren, L., Hu, F., Xiao, J., Wang, J., Tao, M., Zhang, C., Wang, J., et al. (2015). Comparative analysis of testis transcriptomes from triploid and fertile diploid cyprinid fish. Biol Reprod 92, 95.
Ye, L., Zhang, C., Tang, X., Chen, Y., and Liu, S. (2017). Variations in 5S rDNAs in diploid and tetraploid offspring of red crucian carp×common carp. BMC Genet 18, 75.
Zhang, C., He, X.X., Liu, S.J. Sun, Y.D., and Liu, Y. (2005). Chromosome pairing in meiosis I in allotetraploid hybrids and allotriploid crucian carp. Acta Zool Sin 51, 89–94.
Zhang, C., Ye, L., Chen, Y., Xiao, J., Wu, Y., Tao, M., Xiao, Y., and Liu, S. (2015a). The chromosomal constitution of fish hybrid lineage revealed by 5S rDNA FISH. BMC Genet 16, 140.
Zhang, J., Sun, M., Zhou, L., Li, Z., Liu, Z., Li, X.Y., Liu, X.L., Liu, W., and Gui, J.F. (2015b). Meiosis completion and various sperm responses lead to unisexual and sexual reproduction modes in one clone of polyploid *Carassius gibelio*. Sci Rep 5, 10898.
Zhang, Q., and Arai, K. (1999). Aberrant meioses and viable aneuploid progeny of induced triploid loach (*Misgurnus anguillicaudatus*) when crossed to natural tetraploids. Aquaculture 175, 63–76.
Zhu, H.P., Ma, D.M., and Gui, J.F. (2006). Triploid origin of the gibel carp as revealed by 5S rDNA localization and chromosome painting. Chromosome Res 14, 767–776.
Zhu, Y.J., Li, X.Y., Zhang, J., Li, Z., Ding, M., Zhang, X.J., Zhou, L., and Gui, J.F. (2018). Distinct sperm nucleus behaviors between genotypic and temperature-dependent sex determination males are associated with replication and expression-related pathways in a gynogenetic fish. BMC Genomics 19, 437.

SUPPORTING INFORMATION

The supporting information is available online at https://doi.org/10.1007/s11427-020-1900-7. The supporting materials are published as submitted, without typesetting or editing. The responsibility for scientific accuracy and content remains entirely with the authors.